

# On the Noise Stability and Robustness of Adversarially Trained Networks on NVM Crossbars

Deboleena Roy, Chun Tao, Indranil Chakraborty, Kaushik Roy  
*Department of Electrical and Computer Engineering, Purdue University*  
 West Lafayette, USA  
 {roy77, tao88, ichakra, kaushik}@purdue.edu

**Abstract**—Applications based on Deep Neural Networks (DNNs) have grown exponentially in the past decade. To match their increasing computational needs, several Non-Volatile Memory (NVM) crossbar based accelerators have been proposed. Recently, researchers have shown that apart from improved energy efficiency and performance, these approximate hardware also possess intrinsic robustness for defense against Adversarial Attacks, which is an important security concern for DNNs. Prior works have focused on quantifying this intrinsic robustness for vanilla networks, that is DNNs trained on unperturbed inputs. However, adversarial training of DNNs, i.e. training with adversarially perturbed images, is the benchmark technique for robustness, and sole reliance on intrinsic robustness of the hardware may not be sufficient.

In this work, we explore the design of robust DNNs through the amalgamation of adversarial training and the intrinsic robustness offered by NVM crossbar based analog hardware. First, we study the noise stability of such networks on unperturbed inputs and observe that internal activations of adversarially trained networks have lower Signal-to-Noise Ratio (SNR), and are sensitive to noise than vanilla networks. As a result, they suffer significantly higher performance degradation due to the non-ideal computations; on an average  $2\times$  accuracy drop. On the other hand, for adversarial images generated using Projected-Gradient-Descent (PGD) White-Box attacks, ResNet-10/20 adversarially trained on CIFAR-10/100 display a 5 – 10% gain in robust accuracy due to the underlying NVM crossbar when the attack epsilon ( $\epsilon_{\text{attack}}$ , the degree of input perturbations) is greater than the epsilon of the adversarial training ( $\epsilon_{\text{train}}$ ). Our results indicate that implementing adversarially trained networks on analog hardware requires careful calibration between hardware non-idealities and  $\epsilon_{\text{train}}$  to achieve optimum robustness and performance.

**Index Terms**—Adversarial Attacks, Projected Gradient Descent, Adversarial Training, Analog Computing, Non-Volatile Memories, ML acceleration

## I. INTRODUCTION

Today, Deep Neural Networks (DNNs) are the backbone of most Artificial Intelligence (AI) applications and have become the benchmark for a gamut of optimization tasks. These networks, trained using Deep Learning (DL) [1], have demonstrated superlative performance against traditional methods in the fields of Computer Vision [2], Natural Language Processing [3], Recommender Systems [4], etc. Their widespread

usage has spurred rapid innovations in the design of dedicated hardware for such Machine Learning (ML) workloads.

A significant portion of the computations inside a DNN are Matrix Vector Multiplications (MVM). Latest special-purpose accelerators such as GoogleTPU [5], Microsoft BrainWave [6], and NVIDIA V100 [7] improve the MVM operations by co-locating memory and processing elements, and thereby achieve high performance and energy efficiency. However, these accelerators are built on digital CMOS which faces the arduous challenge of scaling saturation [8]. To counter the eventual slowdown of Moore’s Law [9], several Non-Volatile Memory (NVM) technologies such as RRAM [10], PCRAM [11] and spin devices [12] have been developed as promising alternatives. In such emerging technologies, memory is programmed as resistance levels within a device, which are then arranged in a crossbar-like manner. The MVM operations are executed in the analog domain, and it has been shown to significantly reduce power and latency when compared to digital CMOS [13]. In recent years, several NVM crossbar based accelerators have been proposed [14], [15] that leverage this compute efficiency.

While design of specialized ML hardware can address the growing computational needs of DNN-based applications, there still remains several challenges in the ubiquitous adoption of Deep Learning. One of the primary concerns is the susceptibility of DNNs to malicious actors. First noted by [16], now it is widely known that the performance of a DNN can be artificially degraded with carefully designed “Adversarial” inputs. By exploiting the gradient-based learning mechanism, an adversary can generate new data that is nearly indistinguishable from the original data, but it forces the model to classify incorrectly. Such attacks on DNNs are called “Adversarial Attacks” and their strength depends on how much information the attacker has of the model and its training data [17]. Securing the model weights and the training data, and obscuring the gradients of the model itself have been partially effective against such adversaries [18]–[20]. However, the most effective defense against such attacks is “Adversarial Training” [21]–[23], where the model is trained on the adversarial inputs.

When implementing DNNs in any real-world application, both energy efficiency and security play significant roles. Up

The research was funded by C-BRIC, one of six centers in JUMP, a Semiconductor Research Corporation (SRC) program sponsored by DARPA

until recently, research in these two domains have progressed almost independently of each other. In the recent past, there have been several works that explore Algorithm-Hardware co-design opportunities for robust and efficient implementation [24]–[26]. In particular, it has been shown that approximate hardware can provide additional robustness to DNNs by obscuring the true gradients and parameters. While prior works have focused on the robustness gain for models with no other defenses, in this work, we analyze the performance of adversarially trained models on approximate hardware, specifically, NVM crossbars.

When an MVM operation is executed in an NVM crossbar, the output is sensed as a summation of currents through resistive NVM devices. The non-ideal behaviour of the crossbar and its peripheral circuits results in error in the final calculation, and overall performance degradation of the DNN [27], [28]. As these deviations depend on multiple analog variables (voltages, currents, resistances), they are nearly impossible to estimate without a complete model of the architecture and the device parameters, which are difficult for an attacker to obtain. In [26], the authors demonstrated that this non-ideal behaviour can be utilized to obscure the true gradients of the DNN and provide robustness against various types of adversarial attacks. Their analyses of the benefit of intrinsic robustness was limited to vanilla DNNs, i.e. networks trained on the unperturbed, or “clean”, images. However, for a robust DNN implementation, adversarial training is essential. Hence, in this work, we study the performance and robustness of adversarially trained networks when implemented on such NVM crossbars. We observe that adversarial training reduces the noise stability of DNNs, i.e. its ability to withstand perturbations within the network during inference. We also note that the robustness gain from the crossbar is applicable only for certain degrees of attack perturbations. To summarize, our main contributions are:

- We explored the challenges of designing adversarially robust DNNs through the amalgamation of adversarial training and the intrinsic robustness offered by NVM crossbar based analog computing hardware.
- We analyzed the performance of adversarially trained DNNs on NVM crossbars for unperturbed images. Compared against vanilla DNNs (networks trained on unperturbed data), we observed that adversarially trained networks are less noise stable, and hence, suffer greater performance degradation on NVM crossbar based analog hardware.
- For Non-Adaptive Projected-Gradient-Descent White-Box Attacks [21], we demonstrated that the non-idealities provide a gain in robustness when the epsilon of the adversarial attack ( $\epsilon_{attack}$ , the degree of input perturbations) is greater than the epsilon of the adversarial training ( $\epsilon_{train}$ ). In fact, with careful co-design, one can implement a DNN trained with lower  $\epsilon_{train}$  that will have the same or even higher robustness than a DNN trained with a higher  $\epsilon_{train}$  while maintaining a higher natural

test accuracy.

The rest of the paper is organized as follows. In section II-A, we provide a background on NVM crossbar based analog hardware, and in section II-B the prior works on robustness from analog computing is discussed. Next, in section III, we describe in detail the evaluation framework used in our experiments. This is followed by section IV, where we report our findings and discuss the implications. Finally, in section V, we provide the conclusions of our findings.

## II. BACKGROUND AND RELATED WORK

### A. In-Memory Analog Computing Hardware

In-memory analog computing with NVM technologies are being extensively studied for machine learning (ML) workloads [29]–[31] because of their inherent ability to perform efficient matrix-vector multiplications, the key computational kernel in DNNs. The NVM analog compute primitive comprises of a two-dimensional cross-point array with peripheral circuits at the input to provide analog voltages; and peripherals at the output to convert analog currents to digital values, as shown in Fig. 1. At the intersection of horizontally (source-line) and vertically (bit-line) running metal lines, there are NVM devices that can be programmed to discrete number of conductance states [32]. To perform MVM operation using NVM crossbars, analog voltages,  $V_i$ , are applied simultaneously at the source-lines. The multiplication operations are performed between vector  $V_i$  and conductance matrix,  $G_{ij}$ , encoded in each NVM device using the principle of Ohm’s law. Finally, the product,  $V_i G_{ij}$ , representing the resulting current,  $I_{ij}$ , through each NVM device, is summed up using Kirchoff’s current law to produce dot-product outputs,  $I_j$  at each column:

$$I_j = \sum_i I_{ij} = \sum_i V_i G_{ij} \quad (1)$$

As all the columns operate in parallel, NVM crossbars can reduce the  $O(N^2)$  MVM operation between input vector  $V$  and conductance matrix  $G$ , onto  $O(1)$  to produce output vector  $I = VG$ .

Despite the inherent parallelism in NVM crossbars while executing the MVM operation, the computation itself can suffer from errors due to the analog nature of computing. These errors are introduced due to several non-idealities arising from the I-V characteristics of NVM devices, as well as peripheral and parasitic resistances such as  $R_{source}$ ,  $R_{sink}$ ,  $R_{wire}$ , as shown in Fig. 1. The design parameters for NVM crossbars, such as Crossbar Size, ON Resistance etc can have significant impact on the severity of the functional errors introduced by these non-idealities [28]. That is due to the dependence of the effective resistance of a crossbar column on these design parameters. For example, larger crossbar sizes reduce the effective resistance, thus resulting in more errors due to parasitic and peripheral resistances. On the other hand, a higher ON resistance of the device increases the effective resistance, leading to less errors. Overall, these design parameters govern the relationship between the output current

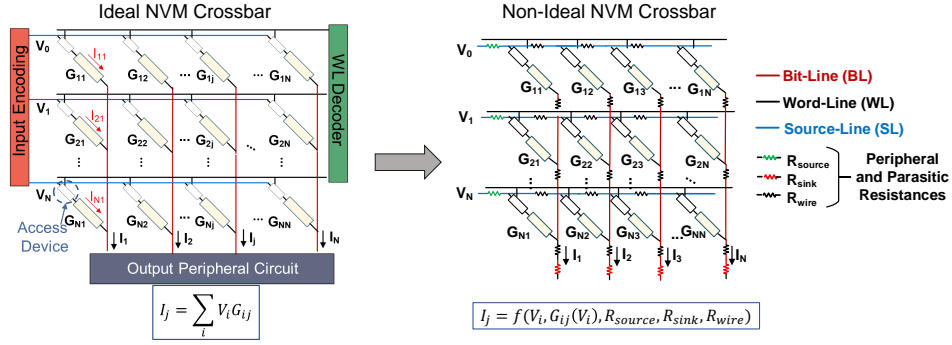


Fig. 1: (Left) Illustration of NVM crossbar which produces output current  $I_j$ , as a dot-product of voltage vector,  $V_i$  and NVM device conductance,  $G_{ij}$ . (Right) Various peripheral and parasitic resistances modify the dot-product computations into an interdependent function of the analog variables (voltage, conductance and resistances) in a non-ideal NVM crossbar.

vector under the influence of non-idealities,  $I_{ni}$ , and the input arguments,  $V$ , and  $G$ . Effectively, in presence of non-idealities in NVM crossbar, the non-ideal output current vector,  $I_{ni}$ , can be expressed as:

$$I_{ni} = f(V, G(V), R_{source}, R_{sink}, R_{wire}) \quad (2)$$

where the conductance matrix  $G(V)$  is a function of  $V$ .

NVM crossbar non-idealities cause deviations in activations of every layer from their expected value. This deviation accumulates as it propagates through the network, and results in degradation in DNN accuracy during inference. Incidentally, such difference in activation and expected value have been also demonstrated to impart adversarial robustness under several kinds of attacks [26].

### B. Adversarial Robustness with Analog Computing

Prior works have shown that various facets of analog computing can be incorporated for adversarial robustness. In [25], the authors use an Optical Processor Unit (OPU) as an analog defense layer. It performs a fixed random transformation, and obfuscates the gradients and the parameters, to achieve adversarial robustness. While [25] used analog processing as an extra layer in their computation, [26] implemented neural networks on an NVM crossbar based analog hardware, and analyzed the impact on accuracy and robustness. They demonstrated two types of Adversarial attacks, one where the attacker is unaware of the hardware (Non-Adaptive Attacks), and the second being Hardware-in-Loop attacks, where the attacker has access to the NVM crossbar. They showed that during Non-Adaptive Attacks on a vanilla DNN, i.e. a network trained on unperturbed images with no other defenses, the gradient obfuscation by the analog hardware provides substantial robustness against both Black Box and White Box Attacks. However, once the attacker gains complete access to the hardware, it can generate Hardware-in-Loop attacks and this significantly diminishes the robustness gain observed earlier. In this work, we further expand the analysis of Non-Adaptive Attacks on adversarially trained DNNs implemented on NVM crossbars.

## III. EVALUATING ADVERSARIALY TRAINED NETWORKS ON NVM CROSSBARS

In this work, we implement adversarially trained DNNs on NVM crossbars based analog hardware and analyze their performance. We first study the effect on natural accuracy, i.e. their performance in the absence of any attack. Analog computations are non-ideal in nature, and the degree of performance degradation depends on the resilience of the DNN to internal perturbations at inference. The degree of performance degradation helps us estimate the noise stability of adversarially trained networks, and understand how they differ from regular networks. Next, we evaluate the performance of these DNNs under adversarial attack and identify the benefit offered by NVM crossbars. Our experimental setup is described in detail in this section.

### A. Datasets and Network Models

We perform our training and evaluation on two image recognition tasks:

- **CIFAR-10** [33]: It is a dataset containing 50,000 training images, and 10,000 test images, each of dimension  $32 \times 32$  across 3 RGB channels. There are total 10 classes. We use two different network architectures for CIFAR-10, a 10-layer ResNet [34], ResNet10w1 and a  $4 \times$  inflated version of it, Resnet10w4 (Table I).
- **CIFAR-100** [33]: This dataset also contains 50,000 training images, and 10,000 test images, each of dimension  $32 \times 32$  across 3 RGB channels, and there are total 100 classes. We use two different network architectures for CIFAR-100, a 20-layer ResNet [34], ResNet20w1 and a  $4 \times$  inflated version of it, ResNet20w4 (Table I).

### B. Adversarial Attacks

We evaluate the DNNs against Non-Adaptive Attacks, where the attacker has no knowledge of the analog hardware, and assumes the DNN is implemented on accurate digital hardware. There exists a variety of attacks depending on how much information about the DNN is available to the attacker. The strongest category of attacks is White-Box Attacks, where the attacker has full knowledge of the DNN weights, inputs and outputs, and we chose this scenario to test our adversarially

TABLE I: ResNet Architectures used for CIFAR-10/100

Group Name	Output Size	CIFAR-10		CIFAR-100	
		ResNet10w1	ResNet10w4	ResNet20w1	ResNet20w4
conv0	$32 \times 32$	$3 \times 3, 16$	$3 \times 3, 16$	$3 \times 3, 16$	$3 \times 3, 16$
conv1	$32 \times 32$	$\begin{bmatrix} 3 \times 3, 16 \\ 3 \times 3, 16 \end{bmatrix} \times 1$	$\begin{bmatrix} 3 \times 3, 64 \\ 3 \times 3, 64 \end{bmatrix} \times 1$	$\begin{bmatrix} 3 \times 3, 16 \\ 3 \times 3, 16 \end{bmatrix} \times 3$	$\begin{bmatrix} 3 \times 3, 64 \\ 3 \times 3, 64 \end{bmatrix} \times 3$
conv2	$16 \times 16$	$\begin{bmatrix} 3 \times 3, 32 \\ 3 \times 3, 32 \end{bmatrix} \times 1$	$\begin{bmatrix} 3 \times 3, 128 \\ 3 \times 3, 128 \end{bmatrix} \times 1$	$\begin{bmatrix} 3 \times 3, 32 \\ 3 \times 3, 32 \end{bmatrix} \times 3$	$\begin{bmatrix} 3 \times 3, 128 \\ 3 \times 3, 128 \end{bmatrix} \times 3$
conv3	$8 \times 8$	$\begin{bmatrix} 3 \times 3, 64 \\ 3 \times 3, 64 \end{bmatrix} \times 2$	$\begin{bmatrix} 3 \times 3, 256 \\ 3 \times 3, 256 \end{bmatrix} \times 2$	$\begin{bmatrix} 3 \times 3, 64 \\ 3 \times 3, 64 \end{bmatrix} \times 3$	$\begin{bmatrix} 3 \times 3, 256 \\ 3 \times 3, 256 \end{bmatrix} \times 3$
Linear	$1 \times 1$	Avg Pool $64 \times 10$	Avg Pool $256 \times 10$	Avg Pool $64 \times 100$	Avg Pool $256 \times 100$

trained DNNs. We use Projected Gradient Descent (PGD) [21] to generate  $l_\infty$  norm bound iterative perturbations, per the eq.:

$$x^{t+1} = \Pi_{x+S}(x^t + \alpha \text{sgn}(\nabla_x L(\theta, x^t, y))) \quad (3)$$

The adversarial example generated at  $(t+1)^{th}$  iteration is represented as  $x^{t+1}$ .  $L(\theta, x, y)$  is the DNN's cost function. It depends on the DNN parameters  $\theta$ , input  $x$ , and labels  $y$ .  $S$  is the set of allowed perturbations, and is defined using the the attack epsilon ( $\epsilon_{attack}$ ) as  $S = \left( \delta | (x + \delta \geq \max(x + \epsilon_{attack}, 0)) \wedge (x + \delta \leq \min(x + \epsilon_{attack}, 255)) \right)$ , where  $x \in [0, 255]$ . The input is an 8-bit image, and every pixel is a value between 0 to 255. For all our experiments, we set the number of iterations to 50. The  $\epsilon_{attack}$  is set within the range [2, 16] and signifies the maximum distortion that can be added to any pixel.

### C. Adversarial Training

First, we train our DNNs on the unperturbed dataset, i.e. "clean" images. We train two DNNs, ResNet10w1 and ResNet10w4 on CIFAR-10, and two DNNs, ResNet20w1 and ResNet20w4 on CIFAR-100. These 4 DNNs are referred to as vanilla DNNs, and form the baseline for our later experiments. Next, we generate adversarially trained DNNs, by using iterative PGD training [21]. At every training step, the batch of clean images is iterated over the network several times to generate a batch of adversarial images, which is then used to update the weights of the network. For a single training procedure, the epsilon of the adversarial image ( $\epsilon_{train}$ ) is fixed, and the iterations is set to 50. For each network architecture in Table I, we generate 4 DNNs, each trained with a different  $\epsilon_{train}$  ([2,4,6,8]) for 200 epochs.

### D. Emulation of the Analog Hardware

In order to evaluate the performance of our adversarially trained DNNs on NVM crossbars in the presence of non-idealities, we need to a) model Equation 2 to express the transfer characteristics of NVM crossbars and b) map the convolutional and fully-connected layers of the workload on a typical spatial NVM crossbar architecture such as PUMA

TABLE II: NVM Crossbar Model Description [28]

NVM Crossbar Model	Crossbar parameters		
	Size	$R_{ON}$ ( $\Omega$ )	$NF$
32x32_100k	32x32	100k	0.14
64x64_100k	64x64	100k	0.26

TABLE III: Functional Simulator precision parameters

Simulation Parameters	CIFAR-10	CIFAR-100
$I_w$	4	4
$W_w$	4	4
$I_{bit}$	16	16
$W_{bit}$	16	16
$I_{i-bit}$	13	12
$W_{i-bit}$	13	12
$O_{bit}$	32	32

[15]. The modelling of Eq. 2 is performed by considering the GENIE<sub>x</sub> [28] crossbar modeling technique which uses a 2-layer perceptron network where the inputs to the network are concatenated  $V$  and  $G$  vectors and the outputs are the non-ideal current,  $I_{ni}$ . The perceptron network is trained using data obtained from HSPICE simulations of NVM crossbars considering the aforementioned non-idealities with different combinations of  $V$  and  $G$  vectors and matrices, respectively.

We generate two crossbar models, 32x32\_100k and 64x64\_100k, their parameters given in Table II. The NVM device used in the crossbar was the the RRAM device model [35]. Each crossbar model has a Non-ideality Factor, defined as,

$$NF = \text{Average} \left( \frac{\text{Output}_{ideal} - \text{Output}_{non-ideal}}{\text{Output}_{ideal}} \right) \quad (4)$$

In our experiments, we consider two crossbar models of different sizes. Higher crossbar size results in higher deviations in computations.

Next, we use a simulation framework, proposed in [28], to map DNN layers on NVM crossbars. Afterwards, we integrate these NVM crossbar models with our PyTorch framework, using the PUMA functional simulator [15], [28], and map DNN layers on NVM crossbars. Such a mapping consists of three segments: i) Lowering, ii) Tiling and iii) Bit Slicing. Lowering refers to dividing the convolutional or linear layer operation into individual MVM operation; Tiling involves distributing bigger MVM operations into smaller crossbar-sized MVM sub-operations. Finally, since each NVM device can only hold upto a limited number of discrete levels, bit-slicing is performed to accommodate MVM operations using large bit-precision inputs and weights. This is done by dividing them into smaller chunks called streams (for inputs) and slices (for weights). We set all precision parameters, given in Table III, for 16 bit fixed point operations, and ensure that for an ideal crossbar behaviour, there is negligible accuracy loss due to reduction in precision. Thus, in our experiments with NVM crossbars any change in performance is solely due to non-ideal behaviour. The bit slicing and fixed-point precision parameters are defined as:

- Input Stream Width ( $I_w$ ) - Bit width of input fragments after slicing.
- Weight Slice Width ( $W_w$ ) - Bit width of weight fragments after slicing.
- Input precision ( $I_{bit}$ ) - Fixed-point precision of the inputs. This is divided into integer bits ( $I_{i-bit}$ ) and fractional bits ( $I_{f-bit}$ ).
- Weight precision ( $W_{bit}$ ) - This refers to fixed-point precision of the weights. This is divided into integer bits and fractional bits ( $W_{f-bit}$ ).
- Output precision ( $O_{bit}$ ) - Fixed-point precision of the outputs of MVM computations.

#### IV. RESULTS

##### A. Noise Stability of Adversarially Trained Networks

At first, we analyze the performance of the vanilla and adversarially trained DNNs on NVM crossbars in the absence of any adversarial attack. We define this accuracy as the Natural Test Accuracy of the DNNs. In Fig. 2, we present a floating column chart where the top of a column represents the accuracy on accurate digital hardware, and where the bottom of the column represents the accuracy on the NVM hardware. The length of the column signifies the drop in accuracy due to non-idealities. Adversarial training, in itself, reduces the natural test accuracy of a DNN, and higher the training epsilon ( $\epsilon_{train}$ ), lower is the test accuracy. When implemented on 2 different NVM crossbar models, 32x32\_100k and 64x64\_100k, the adversarially trained DNNs for all 4 network architectures suffer far greater accuracy degradation than their vanilla counterparts (i.e. DNNs trained on “clean” images). Also, according to Table II, 32x32\_100k has a lower non-ideality factor (NF) compared to 64x64\_100k, i.e. the smaller crossbar has lesser deviations than the larger crossbar. This translates into smaller accuracy drop for 32x32\_100k compared to 64x64\_100k.

On the NVM crossbar model, 32x32\_100k, the average accuracy drop for vanilla DNNs is 3.4% with the maximum of 5.38% for Resnet20w4 on CIFAR-100 dataset (Fig. 2d). Whereas for adversarially trained DNNs, the average is 6.2%, and the maximum drop is 12.44% for ResNet20w1 ( $\epsilon_{train} = 4$ ) on CIFAR-100 dataset (Fig. 2c).

Similarly, for NVM crossbar model, 64x64\_100k, the average accuracy drop for vanilla DNNs is 6.4% with the maximum of 9.83% for Resnet20w4 on CIFAR-100 dataset (Fig. 2d). Whereas for adversarially trained DNNs, the average is 10.3%, and the maximum drop is 20.12% for ResNet20w1 ( $\epsilon_{train} = 4$ ) on CIFAR-100 dataset (Fig. 2c).

Thus, on an average, adversarially trained DNNs suffer  $2\times$  as much performance degradation on NVM crossbar, when compared to vanilla DNNs. To further investigate the cause of this accuracy drop, we look at the output post convolution at every layer of the DNN. To quantify the deviation from ideal, we define two new metrics. The first is Signal to Noise Ratio ( $SNR$ ), and it is defined as,

$$SNR = \log_{10} \left( \sum_N \frac{|Z_{analog}|^2}{|Z_{digital} - Z_{analog}|^2} \right) \quad (5)$$

Here,  $Z$  is the output of a layer before the activation function, i.e. the output right after the MVM operation. The numerator signifies the total signal strength, while the denominator accounts for the noise in the signal, which is the difference between the digital and NVM crossbar implementation.

The second metric is called Noise Sensitivity,  $NS$ , and uses the same definition as in [36],

$$NS = \sum_N \frac{|Z_{digital} - Z_{analog}|^2}{|Z_{digital}|^2} \quad (6)$$

To compute  $SNR$  and  $NS$  we randomly sampled 1000 ( $N$ ) images, i.e. 10% of the total test set for both CIFAR-10 and CIFAR-100, and evaluated the DNNs on 64x64\_100k NVM crossbar model as it has the higher non-ideality factor. In Fig. 3, we observe that for later layers,  $SNR$  of adversarially trained DNNs is lower than that of vanilla networks. In case of CIFAR-10, layers 8-10 of ResNet10w1, and layers 5-10 of ResNet10w4 had lower  $SNR$  for the adversarially trained versions compared to the vanilla version. Similarly, in case of CIFAR-100, layers 11-20 (except layer 18) of both ResNet20w1 and ResNet20w4 have lower  $SNR$  for the adversarially trained versions. Within a DNN, the later layers have greater impact on the classification scores, as they are the closest to the final linear classifier. The lower  $SNR$  indicates that the noise introduced by the NVM non-idealities distorts the MVM outputs for adversarially trained DNNs by a larger margin as compared to the vanilla DNNs. Similarly, in Fig. 4, we observe that the noise sensitivity,  $NS$ , of the corresponding later layers is higher for adversarially trained networks, correlating with the trends of  $SNR$  and accuracy.

Our observations are in line with theoretical and empirical studies of adversarially trained DNNs. The process of adversarial training creates weight transformations that are less noise stable, i.e. given some perturbations at the layer

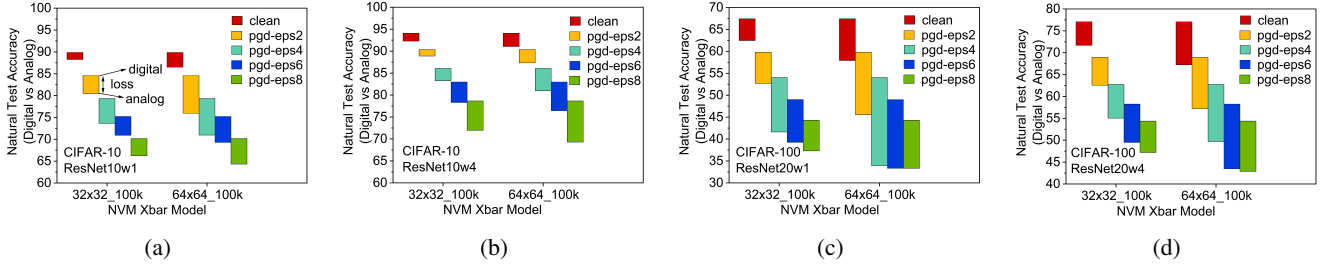


Fig. 2: Digital vs Analog Natural Test Accuracy for vanilla and adversarially trained DNNs. *clean*: vanilla training with unperturbed images. *pgd-epsN*: PGD adversarial training with  $\epsilon_{train} = N = [2, 4, 6, 8]$  and iter = 50

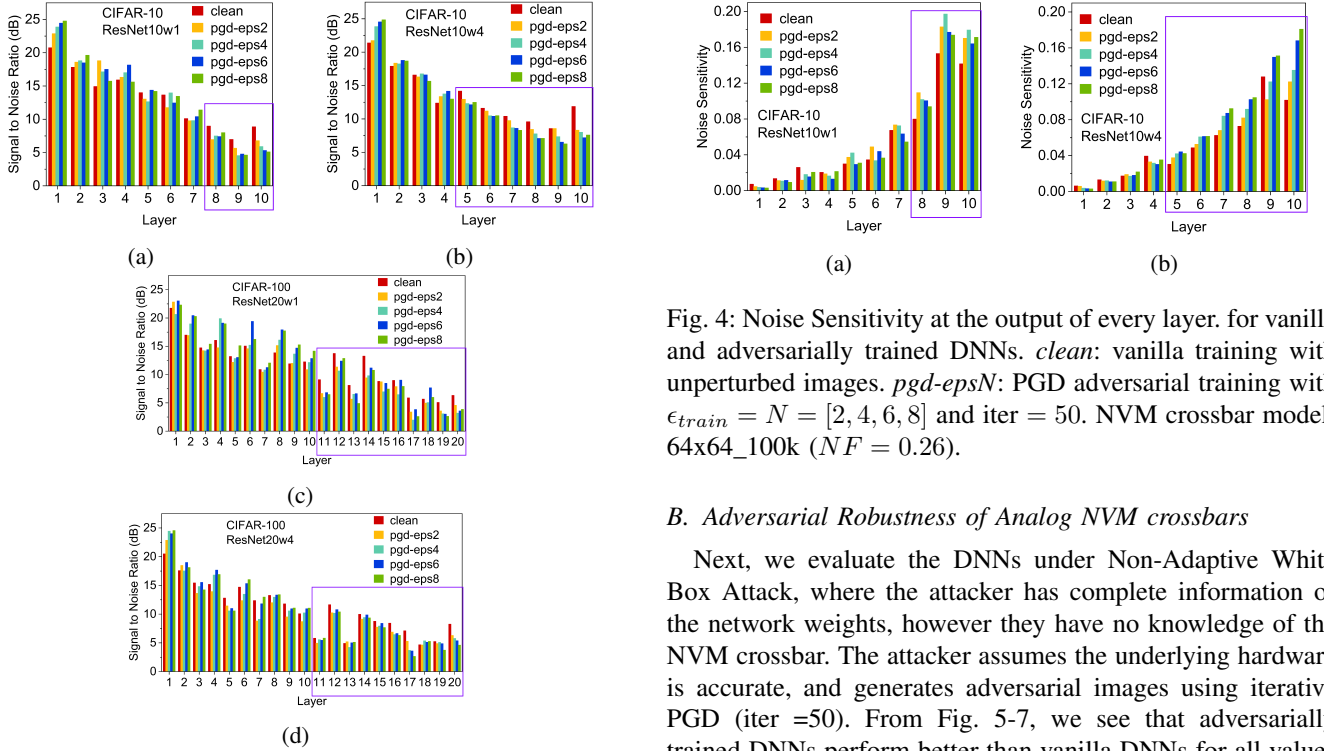


Fig. 3: Signal to Noise ( $SNR$ ) at the output of every layer. for vanilla and adversarially trained DNNs. *clean*: vanilla training with unperturbed images. *pgd-epsN*: PGD adversarial training with  $\epsilon_{train} = N = [2, 4, 6, 8]$  and iter = 50. NVM crossbar model: 64x64\_100k ( $NF = 0.26$ ).

input, it generates greater deviations in the layer output. The optimization landscape of adversarial loss has increased curvature and scattered gradients [37], [38]. The solutions, i.e DNN weights, achieved by the adversarial training often doesn't lie within a stable minima. If one assumes the non-ideal deviations in the NVM crossbar as changes in the weights, then for vanilla DNNs, with stable, flat minimas, these changes have small effect on the loss, and the accuracy drop is low. However, for an adversarially trained DNN, the same degree of changes results in a greater change in loss, and hence greater performance degradation. Thus, this work provides a hardware-backed validation of the complex loss landscape of adversarial training.

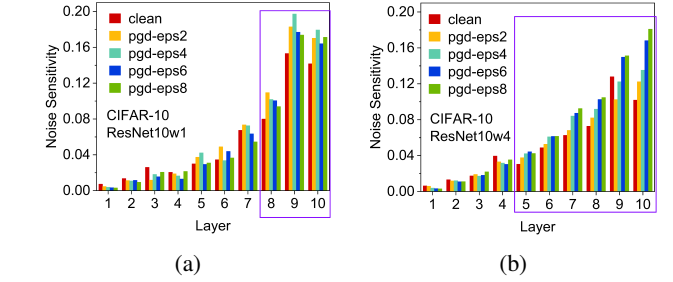


Fig. 4: Noise Sensitivity at the output of every layer. for vanilla and adversarially trained DNNs. *clean*: vanilla training with unperturbed images. *pgd-epsN*: PGD adversarial training with  $\epsilon_{train} = N = [2, 4, 6, 8]$  and iter = 50. NVM crossbar model: 64x64\_100k ( $NF = 0.26$ ).

### B. Adversarial Robustness of Analog NVM crossbars

Next, we evaluate the DNNs under Non-Adaptive White Box Attack, where the attacker has complete information of the network weights, however they have no knowledge of the NVM crossbar. The attacker assumes the underlying hardware is accurate, and generates adversarial images using iterative PGD (iter=50). From Fig. 5-7, we see that adversarially trained DNNs perform better than vanilla DNNs for all values of  $\epsilon_{attack}$ , and in every hardware. Thus, it is imperative to use adversarially trained DNNs to obtain robust implementations.

In Fig. 9 and 10, we plot the net gain in robustness, that is the difference in adversarial accuracy when the same DNN is implemented on an accurate digital hardware and NVM crossbar under the same adversarial attack condition. We observe that for a network trained with  $\epsilon_{train} = N$ , the intrinsic robustness of the network starts having a positive effect only in attacks where  $\epsilon_{attack} > N$ . At  $\epsilon_{attack} = 0$ , i.e in the absence of any attack, the DNNs' accuracy on the analog hardware is significantly lower than digital implementation. As  $\epsilon_{attack}$  is increased, the difference in accuracy slowly reduces, and reaches a tipping point when the  $\epsilon_{attack}$  is equal to  $\epsilon_{train}$ . Beyond that, the analog implementation has a higher accuracy than the digital, i.e. we are in the zone of robustness gain due to the non-idealities. We can draw the following conclusion:

- **The Push-Pull Effect:** As noted in [26], when under adversarial attack, the non-idealities have a dual effect on the accuracy. The first is the loss in accuracy because of inaccurate computations. And the second is the increase



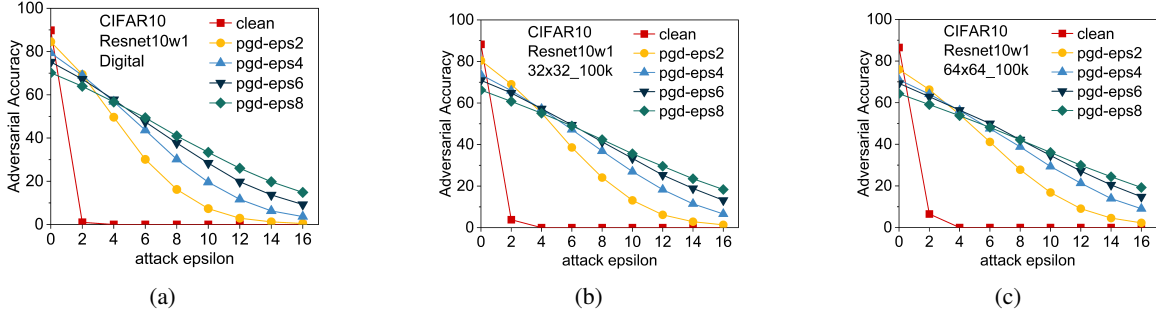


Fig. 5: Adversarial Accuracy under PGD White Box Attack (iter = 50) for ResNet10w1 architecture and CIFAR-10 implemented on 3 different hardware (a) Accurate Digital, (b) NVM crossbar model: 32x32\_100k ( $NF = 0.14$ ), and (c) NVM crossbar model: 64x64\_100k ( $NF = 0.26$ ). *clean*: vanilla training with unperturbed images. *pgd-epsN*: PGD adversarial training with  $\epsilon_{train} = N = [2, 4, 6, 8]$  and iter = 50.

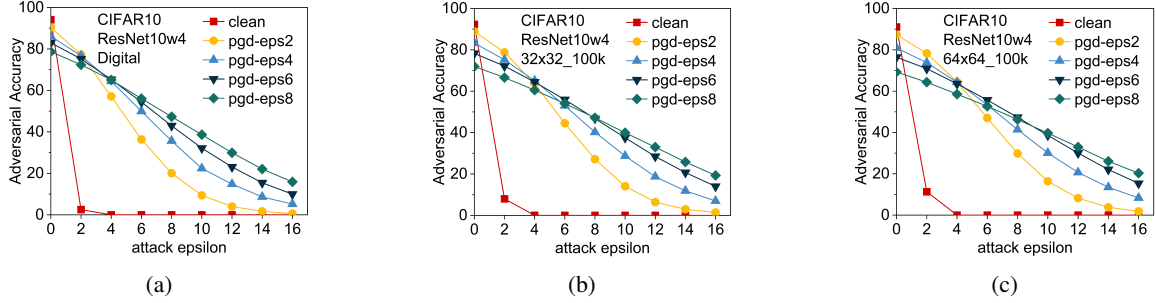


Fig. 6: Adversarial Accuracy under PGD White Box Attack (iter = 50) for ResNet10w4 architecture and CIFAR-10 implemented on 3 different hardware (a) Accurate Digital, (b) NVM crossbar model: 32x32\_100k ( $NF = 0.14$ ), and (c) NVM crossbar model: 64x64\_100k ( $NF = 0.26$ ). *clean*: vanilla training with unperturbed images. *pgd-epsN*: PGD adversarial training with  $\epsilon_{train} = N = [2, 4, 6, 8]$  and iter = 50.

in accuracy due to gradient obfuscation. Because the hardware is unknown to the attacker, the adversarial attacks do not transfer fully to our implementation. At lower  $\epsilon_{attack}$ , the loss due to inaccurate computations is higher, while at higher  $\epsilon_{attack}$ , the intrinsic robustness becomes more significant.

- **Out of Distribution Samples:** In adversarial training, we train DNNs on images with adversarial perturbations bound by the training  $\epsilon_{train}$ . During inference, adversarial images with  $\epsilon_{attack} < \epsilon_{train}$  would have a distribution similar to the training images, and the DNN behaves similar to a vanilla DNN inferring unperturbed images. We only observe accuracy loss due to non-ideal computations. However, adversarial images with  $\epsilon_{attack} > \epsilon_{train}$  are out of distribution with respect to the training data. Now, the DNN is under adversarial attack, and the intrinsic robustness of the NVM crossbar boosts the accuracy.

*Design for Robust DNNs on NVM Crossbars:* When designing robust DNNs on digital hardware, the tradeoff between the adversarial and the natural accuracy of a DNN is fairly straightforward. A higher  $\epsilon_{train}$  during training leads to lowering of natural accuracy, and increase in adversarial accuracy, as shown in Fig. 5(a), 6(a), 7(a), and 8(a). However,

the interplay of non-idealities and adversarial loss creates opportunities for design of DNNs where a DNN trained on lower  $\epsilon_{train}$  can achieve both higher natural accuracy and higher adversarial accuracy, as shown in Fig. 7(b) and (c), and 8(b) and (c). For  $\epsilon_{attack} = [2, 4]$  on 32x32\_100k and for  $\epsilon_{attack} = [2, 4, 6]$  on 64x64\_100k, the ResNet20w1 DNN trained with  $\epsilon_{train} = 2$  performs better or at par than the DNNs trained with higher  $\epsilon_{train}$ . Thus, the non-idealities play a significant role in determining the best DNN within a desired robustness range.

## V. CONCLUSION

NVM crossbars offer intrinsic robustness for defense against Adversarial attacks. While, prior works have quantified these benefits for vanilla DNNs, in this work, we propose design principles of robust DNNs for implementation on NVM crossbar based analog hardware by combining algorithmic defenses such as adversarial training and the intrinsic robustness of the analog hardware. First, we extensively analyze adversarially trained networks on NVM crossbars. We demonstrate that adversarially trained networks are less stable to the non-idealities of analog computing compared to vanilla networks, which impacts their classification accuracy on clean images. Next, we show that under adversarial attack, the gain in accuracy from the non-idealities is conditional on the epsilon

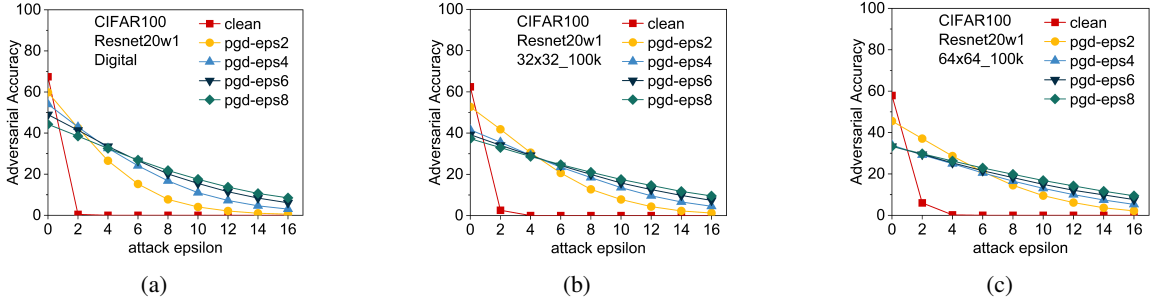


Fig. 7: Adversarial Accuracy under PGD White Box Attack (iter = 50) for ResNet20w1 architecture and CIFAR-100 implemented on 3 different hardware (a) Accurate Digital, (b) NVM crossbar model: 32x32\_100k ( $NF = 0.14$ ), and (c) NVM crossbar model: 64x64\_100k ( $NF = 0.26$ ). *clean*: vanilla training with unperturbed images. *pgd-epsN*: PGD adversarial training with  $\epsilon_{train} = N = [2, 4, 6, 8]$  and iter = 50.

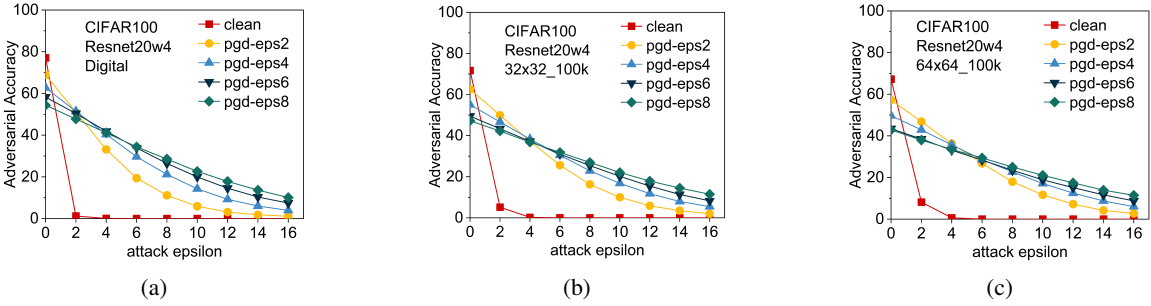


Fig. 8: Adversarial Accuracy under PGD White Box Attack (iter = 50) for ResNet20w4 architecture and CIFAR-100 implemented on 3 different hardware (a) Accurate Digital, (b) NVM crossbar model: 32x32\_100k ( $NF = 0.14$ ), and (c) NVM crossbar model: 64x64\_100k ( $NF = 0.26$ ). *clean*: vanilla training with unperturbed images. *pgd-epsN*: PGD adversarial training with  $\epsilon_{train} = N = [2, 4, 6, 8]$  and iter = 50.

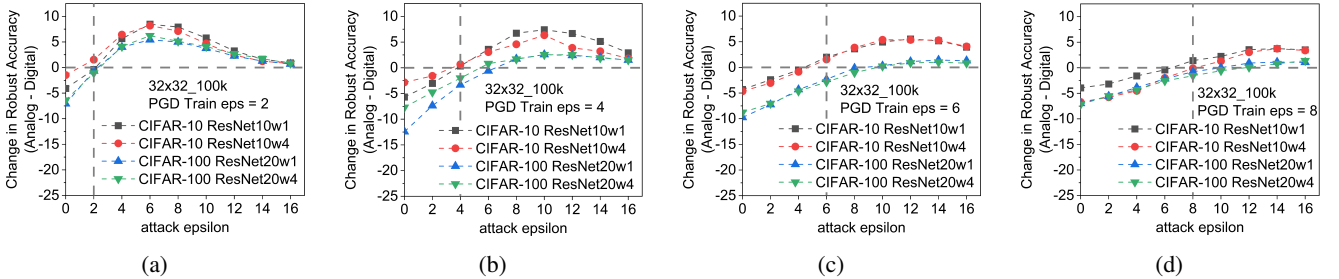


Fig. 9: Difference in Adversarial Accuracy (Robustness Gain = Analog - Digital) for varying PGD Attack ( $\epsilon_{attack}$ ). NVM crossbar model: 32x32\_100k ( $NF = 0.14$ ). 4 network architectures (ResNet10w1, ResNet10w4, ResNet20w1, ResNet20w4) on 2 datasets (CIFAR-10, CIFAR-100) are adversarially trained with (a) PGD,  $\epsilon_{train} = 2$  and iter= 50 (b) PGD,  $\epsilon_{train} = 4$  and iter= 50 (c) PGD,  $\epsilon_{train} = 6$  and iter= 50 (d) PGD,  $\epsilon_{train} = 8$  and iter= 50

of the attack ( $\epsilon_{attack}$ ) being greater than the epsilon used during adversarial training ( $\epsilon_{train}$ ). By implementing on NVM crossbar based analog hardware, a DNN trained with lower  $\epsilon_{train}$  will have the same or even higher robustness than a DNN trained with a higher  $\epsilon_{train}$  while maintaining a higher natural test accuracy. This work paves the way for a new paradigm of hardware-algorithm co-design which incorporates both energy-efficiency and adversarial robustness.

## REFERENCES

- [1] I. Goodfellow, Y. Bengio, A. Courville, and Y. Bengio, *Deep learning*. MIT press Cambridge, 2016, vol. 1, no. 2.
- [2] A. Voulodimos *et al.*, “Deep learning for computer vision: A brief review,” *Computational intelligence and neuroscience*, vol. 2018, 2018.
- [3] T. Young *et al.*, “Recent trends in deep learning based natural language processing [review article],” *IEEE Computational Intelligence Magazine*, vol. 13, no. 3, pp. 55–75, 2018.
- [4] H.-T. Cheng *et al.*, “Wide & deep learning for recommender systems,” in *Proceedings of the 1st workshop on deep learning for recommender systems*, 2016, pp. 7–10.
- [5] N. P. Jouppi *et al.*, “In-datacenter performance analysis of a tensor pro-



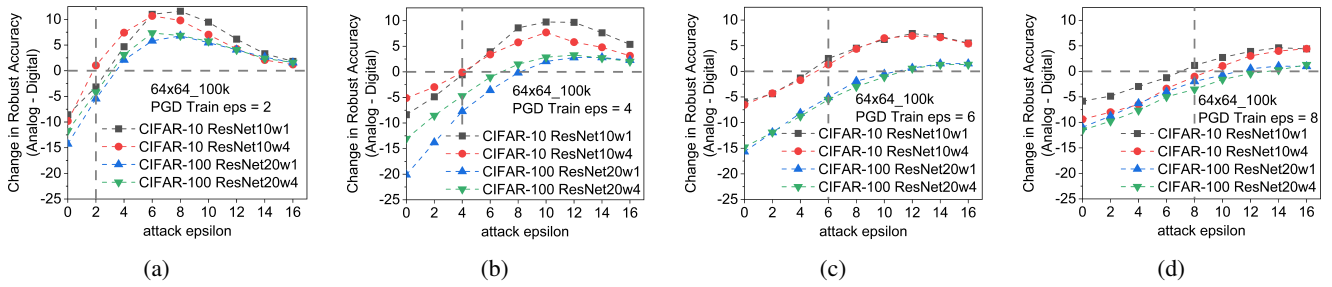


Fig. 10: Difference in Adversarial Accuracy (Robustness Gain = Digital - Analog) for varying PGD Attack ( $\epsilon_{attack}$ ). NVM crossbar model: 64x64\_100k ( $NF = 0.26$ ). 4 network architectures (ResNet10w1, ResNet10w4, ResNet20w1, ResNet20w4) on 2 datasets (CIFAR-10, CIFAR-100) are adversarially trained with (a) PGD,  $\epsilon_{train} = 2$  and iter= 50 (b) PGD,  $\epsilon_{train} = 4$  and iter= 50 (c) PGD,  $\epsilon_{train} = 6$  and iter= 50 (d) PGD,  $\epsilon_{train} = 8$  and iter= 50

cessing unit,” in *2017 ACM/IEEE 44th Annual International Symposium on Computer Architecture (ISCA)*. IEEE, 2017, pp. 1–12.

- [6] E. Chung *et al.*, “Serving dnns in real time at datacenter scale with project brainwave,” *IEEE Micro*, vol. 38, no. 2, pp. 8–20, 2018.
- [7] “Nvidia tesla v100 gpu architecture, the world’s most advanced data center gpu,” NVIDIA Corporation, Tech. Rep., 2017.
- [8] X. Xu *et al.*, “Scaling for edge inference of deep neural networks,” *Nature Electronics*, vol. 1, no. 4, pp. 216–222, 2018.
- [9] R. R. Schaller, “Moore’s law: past, present and future,” *IEEE spectrum*, vol. 34, no. 6, pp. 52–59, 1997.
- [10] H.-S. P. Wong *et al.*, “Metal–oxide rram,” *Proceedings of the IEEE*, vol. 100, no. 6, pp. 1951–1970, 2012.
- [11] —, “Phase change memory,” *Proceedings of the IEEE*, vol. 98, no. 12, pp. 2201–2227, 2010.
- [12] X. Fong *et al.*, “Spin-transfer torque devices for logic and memory: Prospects and perspectives,” *IEEE TCAD*, vol. 35, no. 1, pp. 1–22, 2015.
- [13] I. Chakraborty *et al.*, “Resistive crossbars as approximate hardware building blocks for machine learning: Opportunities and challenges,” *Proceedings of the IEEE*, 2020.
- [14] A. Shafiee *et al.*, “Isaac: A convolutional neural network accelerator with in-situ analog arithmetic in crossbars,” *ACM SIGARCH Computer Architecture News*, vol. 44, no. 3, pp. 14–26, 2016.
- [15] A. Ankit *et al.*, “Puma: A programmable ultra-efficient memristor-based accelerator for machine learning inference,” in *Proceedings of the Twenty-Fourth International Conference on Architectural Support for Programming Languages and Operating Systems*, 2019, pp. 715–731.
- [16] C. Szegedy, W. Zaremba, I. Sutskever, J. Bruna, D. Erhan, I. Goodfellow, and R. Fergus, “Intriguing properties of neural networks,” in *International Conference on Learning Representations*, 2014. [Online]. Available: <http://arxiv.org/abs/1312.6199>
- [17] I. Goodfellow, J. Shlens, and C. Szegedy, “Explaining and harnessing adversarial examples,” in *International Conference on Learning Representations*, 2015. [Online]. Available: <http://arxiv.org/abs/1412.6572>
- [18] G. S. Dhillon, K. Azizzadenesheli, Z. C. Lipton, J. D. Bernstein, J. Kossai, A. Khanna, and A. Anandkumar, “Stochastic activation pruning for robust adversarial defense,” in *International Conference on Learning Representations*, 2018.
- [19] J. Buckman *et al.*, “Thermometer encoding: One hot way to resist adversarial examples,” in *International Conference on Learning Representations*, 2018.
- [20] A. Athalye *et al.*, “Obfuscated gradients give a false sense of security: Circumventing defenses to adversarial examples,” *arXiv preprint arXiv:1802.00420*, 2018.
- [21] A. Madry, A. Makelov, L. Schmidt, D. Tsipras, and A. Vladu, “Towards deep learning models resistant to adversarial attacks,” in *International Conference on Learning Representations*, 2018.
- [22] A. Shafahi, M. Najibi, A. Ghiasi, Z. Xu, J. Dickerson, C. Studer, L. S. Davis, G. Taylor, and T. Goldstein, “Adversarial training for free!” *Advances in Neural Information Processing Systems* 32, vol. 5, pp. 3358–3369, 2019.
- [23] E. Wong, L. Rice, and J. Z. Kolter, “Fast is better than free: Revisiting adversarial training,” in *International Conference on Learning Representations*, 2019.
- [24] A. Guesmi, I. Alouani, K. N. Khasawneh, M. Baklouti, T. Frikha, M. Abid, and N. Abu-Ghazaleh, “Defensive approximation: securing cnns using approximate computing,” in *Proceedings of the 26th ACM International Conference on Architectural Support for Programming Languages and Operating Systems*, 2021, pp. 990–1003.
- [25] A. Cappelli, R. Ohana, J. Launay, L. Meunier, I. Poli, and F. Krzakala, “Adversarial robustness by design through analog computing and synthetic gradients,” *arXiv preprint arXiv:2101.02115*, 2021.
- [26] D. Roy, I. Chakraborty, T. Ibrayev, and K. Roy, “On the intrinsic robustness of nvm crossbars against adversarial attacks,” *arXiv preprint arXiv:2008.12016*, 2020.
- [27] I. Chakraborty *et al.*, “Technology aware training in memristive neuromorphic systems for nonideal synaptic crossbars,” *IEEE TETCI*, vol. 2, no. 5, pp. 335–344, 2018.
- [28] I. Chakraborty, M. Fayezi Ali, D. Eun Kim, A. Ankit, and K. Roy, “Geniex: A generalized approach to emulating non-ideality in memristive xbars using neural networks,” in *2020 57th ACM/IEEE Design Automation Conference (DAC)*, 2020, pp. 1–6.
- [29] G. W. Burr *et al.*, “Experimental demonstration and tolerancing of a large-scale neural network (165 000 synapses) using phase-change memory as the synaptic weight element,” *IEEE Transactions on Electron Devices*, vol. 62, no. 11, pp. 3498–3507, 2015.
- [30] S. Ambrogio *et al.*, “Equivalent-accuracy accelerated neural-network training using analogue memory,” *Nature*, vol. 558, no. 7708, p. 60, 2018.
- [31] F. Cai *et al.*, “A fully integrated reprogrammable memristor–cmos system for efficient multiply–accumulate operations,” *Nature Electronics*, vol. 2, no. 7, pp. 290–299, 2019.
- [32] M. Hu *et al.*, “Dot-product engine for neuromorphic computing: programming 1t1m crossbar to accelerate matrix-vector multiplication,” in *Design Automation Conference (DAC)*, 2016 53rd ACM/EDAC/IEEE. IEEE, 2016, pp. 1–6.
- [33] A. Krizhevsky *et al.*, “Learning multiple layers of features from tiny images,” 2009.
- [34] K. He *et al.*, “Deep residual learning for image recognition,” in *Proceedings of the IEEE conference on computer vision and pattern recognition*, 2016, pp. 770–778.
- [35] X. Guan *et al.*, “A spice compact model of metal oxide resistive switching memory with variations,” *IEEE electron device letters*, vol. 33, no. 10, pp. 1405–1407, 2012.
- [36] S. Arora, R. Ge, B. Neyshabur, and Y. Zhang, “Stronger generalization bounds for deep nets via a compression approach,” in *International Conference on Machine Learning*. PMLR, 2018, pp. 254–263.
- [37] E. Duesterwald, A. Murthi, G. Venkataraman, M. Sinn, and D. Vijaykeerthy, “Exploring the hyperparameter landscape of adversarial robustness,” *arXiv preprint arXiv:1905.03837*, 2019.
- [38] C. Liu, M. Salzmann, T. Lin, R. Tomioka, and S. Süssstrunk, “On the loss landscape of adversarial training: Identifying challenges and how to overcome them,” *Advances in Neural Information Processing Systems*, vol. 33, 2020.